Pressure-driven orbital selective insulator-to-metal transition and spin-state crossover in cubic CoO

Li Huang,[1,2] Yilin Wang,[1] and Xi Dai[1]

[1]*Beijing National Laboratory for Condensed Matter Physics, and Institute of Physics, Chinese Academy of Sciences, Beijing 100190, China*

[2]*Science and Technology on Surface Physics and Chemistry Laboratory, P.O. Box 718-35, Mianyang 621907, Sichuan, China*

(Received 18 December 2011; revised manuscript received 22 April 2012; published 12 June 2012)

The metal-insulator and spin state transitions of CoO under high pressure are studied by using density functional theory combined with dynamical mean-field theory. Our calculations predict that the metal-insulator transition in CoO is a typical orbital selective insulator-to-metal transition, where the t_{2g} orbitals of a Co 3*d* shell become metallic first around 60 GPa while the e_g orbitals still remain insulating until 170 GPa. Further studies of the spin states of a Co 3*d* shell reveal that the orbital selective Mott phase in the intermediate pressure regime is mainly stabilized by the high-spin state of the Co 3*d* shell, and the transition from this phase to the fully metallic state is driven mainly by the high-spin to low-spin transition of the Co^{2+} ions. Our results are in good agreement with the most recent transport and x-ray emission experiments under high pressure.

DOI: 10.1103/PhysRevB.85.245110 PACS number(s): 71.30.+h, 71.27.+a, 75.30.Wx, 91.60.Gf

I. INTRODUCTION

Although the Mott metal-insulator transition (MIT) has been studied extensively for decades, most of the work has been focused on the single-band Hubbard model, where the Mott transition is driven completely by the ratio of the local Coulomb interaction and bandwidth. However, most of the Mott MITs in realistic materials[1] involve more than one band where the transitions are driven not only by the local Coulomb interaction but also by the distribution of the electrons among these bands. For example, the redistribution of the four electrons among three bands may lead to a so-called orbital selective Mott transition (OSMT)[2–7] in these bands. On the other hand, in many systems the redistribution of the electrons among different bands is induced by the crossover in spin states, i.e., the high-spin (HS) to low-spin (LS) transition.[8] Therefore, in realistic materials (e.g., 3*d* transition metal compounds) the Mott MITs and spin state crossovers are closely related to each other.[9–15]

Recently, the high-pressure experiments on charge transfer insulator CoO revealed very interesting behaviors in both transport properties and x-ray emission spectroscopy (XES). The transport measurement[16] indicated that with the increment of pressure, there are two transitions in resistivity. One happens around 60 GPa and the other takes place around 130 GPa. However, room-temperature XES measurements[17,18] on similar samples show that the spin states of Co^{2+} ions persist in the HS state all the way to 140 GPa, after which the crossover from HS to LS states happens. Hence the interplay between the HS-LS transition and the two-step metal-insulator transition becomes the key factor to understand the underlying physics in CoO.

The pressure-driven MITs and magnetic moment collapses in transition metal oxides have been studied extensively using first-principles calculations.[9–11,13,19,20] With regard to CoO, its magnetic state transition under pressure was first discussed by Cohen *et al.*[13] within the Stoner scenario by employing the local spin density approximation (LSDA) and generalized gradient approximation (GGA) approaches of density functional theory. A transition from HS to a nonmagnetic metallic state was found around 88 GPa. Since these calculations did not take the correlation effects of the Co 3*d* shell into account, the experimentally observed excitation gap for CoO (Ref. 18) as large as 1.8–2.6 eV was not reproduced completely. Recently, Zhang *et al.*[21] reinvestigated the pressure-driven magnetic phase transition in CoO by using the LSDA + *U* approach. The HS-LS transition is indeed obtained to be of $t_{2g}^5 e_g^2 \rightarrow t_{2g}^6 e_g^1$ character, but the electronic structure transition is an insulator-to-insulator scheme. This scenario contradicts the resistivity data under high pressure,[16] which show dramatic changes in resistivity indicating the insulator-to-metal transition with pressure.

In this paper, based on the local density approximation (LDA) combined with dynamical mean-field theory (DMFT),[22,23] we have carried out theoretical calculations for cubic phase CoO at different volumes. Our calculations show that CoO under pressure is a typical system which exhibits OSMT. At ambient pressure, our calculation yields a correct charge transfer insulator phase for CoO with an energy gap being around 1.8 eV. At the first transition around 60 GPa, the t_{2g} bands of the Co 3*d* shell become metallic while the e_g bands still remain insulating until the pressure reaches 170 GPa. Therefore, in CoO the exotic orbital selective Mott phase (OSMP) with metallic t_{2g} and insulating e_g bands is stable in quite a large pressure window between 60 and 170 GPa. Our LDA + DMFT calculations also find that the Co^{2+} ions remain in a HS state during the first transition and the crossover to the LS state starts only after the second transition, which is in good agreement with both the resistivity[16] and XES data[17,18] for CoO.

II. METHOD

The LDA + DMFT calculations[24–26] in the present paper have been carried out by using the pseudopotential plane-wave method with the QUANTUM ESPRESSO package[27] for the LDA part and continuous-time quantum Monte Carlo (CTQMC)[28,29] as the impurity solver for the DMFT part. For the ground state calculations, the norm-conserved-type pseudopotentials for Co and O species that we constructed are adopted, the cutoff energy for the plane-wave expansion is 60 Ha, and the *k*-mesh for the Brillouin zone integration is $12 \times 12 \times 12$. These pseudopotentials and computational parameters are carefully checked and tuned to ensure the numerical convergences. The single-particle low energy effective Hamiltonian is obtained by applying a projection

onto atomic-centered symmetry-constrained Wannier function (WF) orbitals including all the Co $3d$ and oxygen $2p$ orbitals, as is described in detail in Ref. 24. That would correspond to an 8×8 p-d Hamiltonian which is a minimal model required for a correct description of the electronic structure of CoO due to its charge transfer nature.[1]

The LDA + DMFT calculations presented below have been done for crystal volumes corresponding to values of pressure up to 280 GPa. For simplicity, all first-principles calculations are performed in a paramagnetic configuration for rocksalt-type crystal structure with the lattice constant scaled to give a volume corresponding to applied pressure. The Coulomb interaction is taken into account merely among Co $3d$ orbitals. In the present work, we choose $U = 8.0$ and $J = 0.9$ eV, which are close to previous estimations.[21,30] We adopt the scheme proposed in Ref. 11 to deal with the double counting energy. The effective impurity problem for the DMFT is solved by the CTQMC quantum impurity solver (hybridization expansion version) supplemented with the recently developed orthogonal polynomial representation algorithm.[31] Calculations for all crystal volumes are performed in a paramagnetic state at a temperature of 290 K, which is slightly higher than the Néel temperature $T_N = 289$ K.[33] During the Monte Carlo simulations, except for the traditional local updates, global updates such as swap spin-up and spin-down states are done every 20 000 Monte Carlo sweeps to ensure the ergodicity, and the final results are symmetrized to ensure the paramagnetic solutions. Finally, the maximum entropy method[32] is used to perform analytical continuation to obtain the impurity spectral functions of Co $3d$ states.

III. RESULTS AND DISCUSSION

In Fig. 1, the evolution of the single-particle spectral function for Co $3d$ states upon compression is shown. The

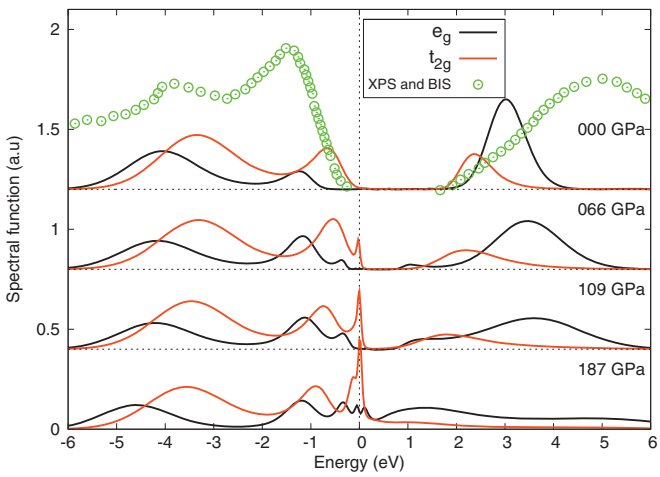

FIG. 1. (Color online) Single-particle spectral function of Co $3d$ states vs pressure obtained in LDA + DMFT calculations at 290 K. The spectral function is obtained from the imaginary-time Green function $G(\tau)$ by using the maximum entropy method,[32] and the results are cross-checked by using the recently developed stochastic analytical continuation method.[34] The available x-ray photoelectron spectroscopy (XPS) and bremsstrahlung isochromat spectroscopy (BIS) experimental data[18] are drawn in this figure as a comparison.

momentum-integrated spectral function $A(\omega)$ under ambient pressure shows well defined insulating behavior for all $3d$ orbitals. However, the energy gap for e_g orbitals is slightly larger than that for t_{2g} states, indicating that the latter orbitals are closer to MIT than the former ones. At zero pressure, the calculated gaps for t_{2g} orbitals of about 1.8 eV and for e_g orbitals of about 2.5 eV agree well with the recent XPS/BIS experimental value of 1.8 eV.[18] The LDA + DMFT calculations done for small volume values corresponding to high pressures yield a metallic state for CoO starting from 60 GPa, in agreement with room-temperature resistivity data.[16] One can see that t_{2g} orbitals become metallic whereas e_g orbitals still remain insulating. This behavior is reminiscent of the OSMT scenario as discovered first in ruthenates.[2] The spectral functions for t_{2g} orbitals in Fig. 1 for pressure values larger than 60 GPa become typical for strongly correlated metal close to MIT, namely well-pronounced Hubbard bands and a narrow quasiparticle peak. However, the $A(\omega)$ for e_g orbitals remains insulating with Hubbard bands only but the gap size is strongly reduced compared with that of ambient pressure. When the pressure exceeds about 170 GPa (see Fig. 2), the e_g states undergo an insulator-to-metal transition. As is seen in Fig. 1, at 187 GPa the insulator gaps for both $3d$ orbitals disappear finally.

In order to reveal the nature of OSMT in Co $3d$ orbitals upon compression, we make a further estimation for their quasiparticle weights by using the well-known equation[22] $Z^{-1} = 1 - \frac{\partial}{\partial\omega}\mathrm{Re}\Sigma(\omega)|_{\omega=0}$, where $\mathrm{Re}\Sigma(\omega)$ is the real part of the impurity self-energy function at real frequency axis. In Fig. 2(a), the calculated quasiparticle weights for t_{2g} and e_g states as a function of pressure are shown. It is apparent that the phase diagram can be split vertically into three different zones: (i) $0 < P < 60$ GPa. The quasiparticle weights for both the e_g and t_{2g} orbitals approach zero, and the system exhibits completely insulating behavior. (ii) $60 < P < 170$ GPa. The quasiparticle weights for t_{2g} states become considerable, whereas those for e_g states remain very tiny. At this range of pressure, it gives an exotic OSMP. (iii) $P > 170$ GPa. The quasiparticle weights for both t_{2g} and e_g states show a dramatic increment with pressure, and finally the system goes into a fully metallic state. While Z specifies the quasiparticle weight of the band right at E_F, the imaginary-time Green function at $\tau = \frac{\beta}{2}$ represents the integrated spectral weight within a few k_BT of E_F.[3] So to confirm the calculated results of quasiparticle weights, further analysis of $G(\frac{\beta}{2})$ is done. The normalized $G(\frac{\beta}{2})$ are illustrated in Fig. 2(b). Clearly, the first MIT occurs around 60 GPa and the second transition occurs around 170 GPa, which is consistent with the transition points obtained by previous analysis.

In Fig. 3, we show the evolution of Co $3d$ occupancies (upper panel) and the atomic state probability (lower panel) under compression. Due to the charge transfer from O $2p$ orbitals to Co $3d$ orbitals, the total $3d$ state's occupation number is ~7.2, which is slightly larger than the nominal value 7.0. At ambient pressure, the occupation numbers for t_{2g} and e_g orbitals are $n(e_g) = 0.54$ and $n(t_{2g}) = 0.84$, respectively. Those numbers agree very well with the HS state of the Co^{2+} ion in a cubic crystal field with two electrons in e_g states and five electrons in t_{2g} states ($t_{2g}^5 e_g^2$ character, $S = 3/2$). Over the pressure range from 0 to 170 GPa, the occupation numbers for $3d$ orbitals basically remain unchanged. When the pressure is

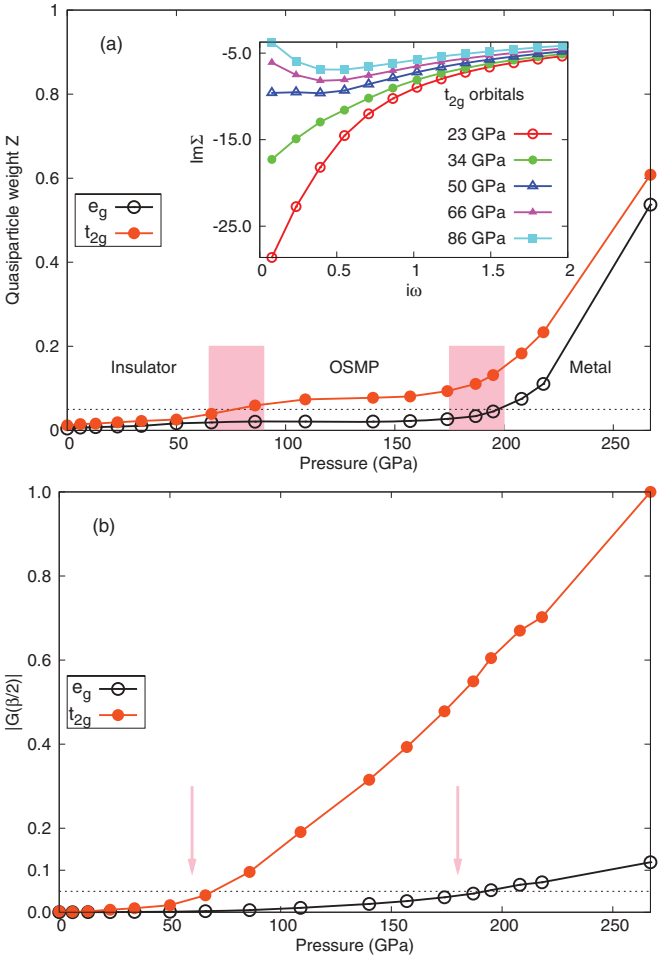

FIG. 2. (Color online) (a) Quasiparticle weight Z of Co $3d$ states as a function of pressure. The label OSMP denotes the orbital selective Mott phase. The transition zones are highlighted by pink vertical bars. Inset: $\mathrm{Im}\Sigma(i\omega)$ of t_{2g} orbitals under various pressures. (b) The corresponding imaginary-time Green function at $\tau = \frac{\beta}{2}$ as a function of pressure. In this figure, the normalized quantities by $G(\frac{\beta}{2})$ at 267 GPa are shown and the arrows correspond to phase transition points.

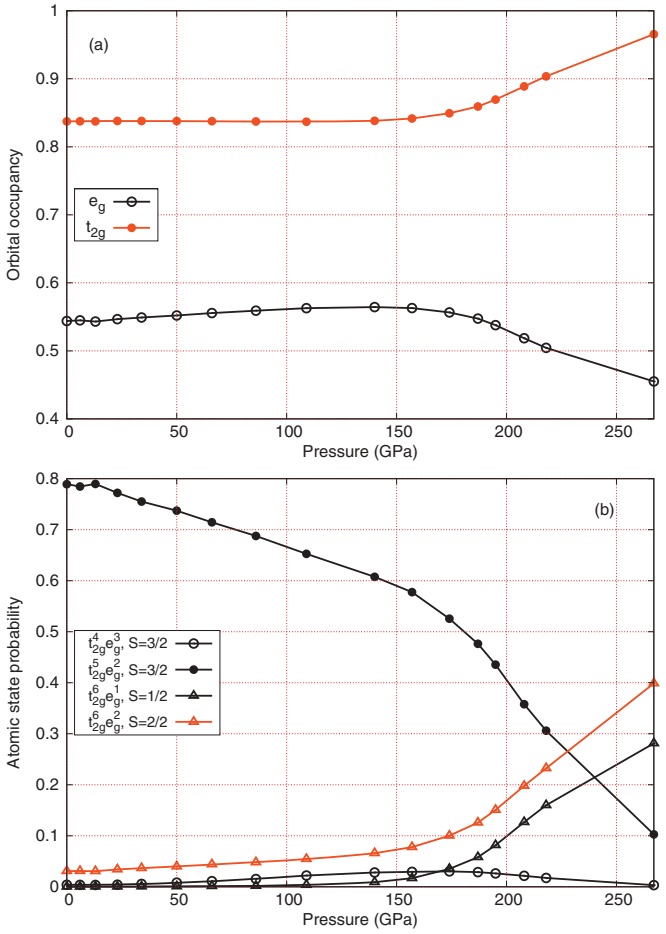

FIG. 3. (Color online) (a) The orbital occupancy of Co $3d$ states as a function of external pressure. (b) The principal pressure-dependent atomic state probabilities of Co $3d$ states obtained by LDA + DMFT calculations.

larger than 170 GPa, the occupation numbers for t_{2g} and e_g states show a dramatic change. The $n(t_{2g})$ increases from 0.84 to 1.0 and $n(e_g)$ decreases from 0.54 to 0.25 eventually, which agrees well with the LS configuration of the Co^{2+} ion ($t_{2g}^6 e_g^1$ character, $S = 1/2$). Thus the evolution of Co $3d$ occupancies with respect to external pressure provides very strong evidence for the HS-LS spin state crossover in cubic CoO.

During the Monte Carlo simulation, we keep track of the different atomic state configurations visited and draw them as histograms, which give complementary information on the variations of occupancies and magnetic states. In Fig. 3(b), we show the probabilities for several uppermost $N = 7$ and 8 atomic state configurations. It is apparent that at ambient pressure, the HS state ($t_{2g}^5 e_g^2$ character, $S = 3/2$) makes a predominant contribution and the contributions from the LS state ($t_{2g}^6 e_g^1$ character, $S = 1/2$) and the intermediate spin (IS) state ($t_{2g}^6 e_g^2$ character, $S = 2/2$) can be ignored reasonably. Upon increasing the pressure, the contributions from the HS state have dropped, and those from the LS and IS states have tended to grow, and the total spin magnetic moment will decrease as well (see Fig. 4). We note that except for the $t_{2g}^5 e_g^2$ configuration, the contribution from another HS configuration $t_{2g}^4 e_g^3$ ($S = 3/2$) is very little. Thus it is confirmed that the HS-LS spin state transition for CoO mainly has a $t_{2g}^5 e_g^2 \rightarrow t_{2g}^6 e_g^1$ character, which is consistent with previous assumptions.[17,21] In addition, it should be pointed out that the contribution to magnetic collapse in CoO from the HS-IS spin state transition ($t_{2g}^5 e_g^2 \rightarrow t_{2g}^6 e_g^2$ character) cannot be neglected as well.

Next, we concentrate our attention on the magnetic properties of cubic CoO under pressure. Figure 4(a) shows the evolution of the local spin magnetic moment with external pressure. We note that the effective local moment M_e is defined through the local spin susceptibility $\sqrt{T\chi_{\mathrm{loc}}}$, where χ_{loc} is defined as $\chi_{\mathrm{loc}} = \int_0^\beta d\tau \chi_{\mathrm{loc}}(\tau) = \int_0^\beta d\tau \langle S_z(0) S_z(\tau)\rangle$. As is clearly seen in Fig. 4(a), under compression the local moment decreases slightly from its ambient pressure HS value down to about 170 GPa. Further compression rapidly degrades the moment, which is accompanied by a redistribution of electrons $e_g \rightarrow t_{2g}$ within the Co $3d$ shell (see Fig. 3). As is clearly shown in this figure, under low pressure our results coincide very well with previously published theoretical data.[13,20]

In Fig. 4(b), the spin-spin correlation functions $\chi_{\mathrm{loc}}(\tau)$ under various external pressure values are illustrated. For

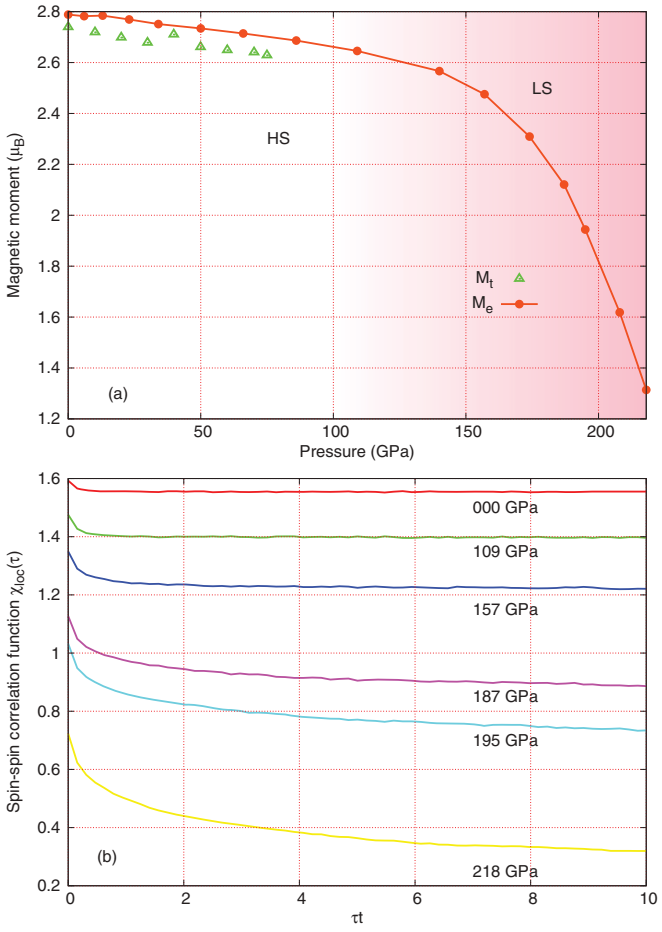

FIG. 4. (Color online) Spin state transition in CoO. (a) Evolution of the local spin magnetic moment of Co 3d states. Here M_e denotes effective local moment, which can be calculated by $\sqrt{T\chi_{\rm loc}}$, and M_t (illustrated by triangle) denotes the previous theoretical results.[20] (b) Spin-spin correlation function $\chi_{\rm loc}(\tau) = \langle S_z(0)S_z(\tau)\rangle$ obtained by LDA + DMFT calculations under various external pressures.

high pressure, a Fermi liquid phase (LS state) is identified. On the other hand, for low pressure, CoO exhibits a well-defined frozen moment phase (HS state). In the Fermi liquid phase, the spin-spin correlation function behaves as $\chi(\tau) \sim [T/\sin(T\tau\pi)]^2$ for times τ sufficiently far from $\tau = 0$ or β, respectively. For $P \geqslant 170$ GPa, it displays significant Fermi liquid behaviors, which is consistent with the obtained OSMT phase diagram (see Fig. 2) for CoO. The frozen moment phase is characterized by a spin-spin correlation function that approaches nonzero constants at large τ, as is easily seen from 0 to 170 GPa. Thus this figure reveals a phase transition between a LS Fermi liquid metallic phase and a HS phase with frozen moments again.

Now we discuss the most interesting issue of this paper, namely the relationship between OSMT and the HS-LS transition. The detailed analysis of the spin state indicates that the HS-LS spin state transition is the most important driving force for the OSMT in CoO. Once the Co^{2+} ions stay in a HS state, the e_g bands are always half-filled, which greatly favors the Mott insulator phase and makes it very hard for the e_g bands to become metallic. On the other hand, in the HS state the filling factor of t_{2g} bands is only 1/6 (in terms of hole density), which makes it much easier for them to become metallic. For example, the previous studies on the multiband Hubbard model[35] show that the critical U_c for the half-filled two-band model is around $1.7W$, and that of the 1/6 filling three-band model is around $3.0W$, where W is the bandwidth. Thus apparently it is the different situation in filling factors between e_g and t_{2g} bands which makes the two subshells behave so differently under pressure. Once the LS state is stabilized above 170 GPa, the e_g orbitals are no longer half-filled and they turn to the metallic phase eventually.

Finally, although our LDA + DMFT calculations in the present paper are only for the room-temperature paramagnetic phase, we can still get some useful insights for the possible magnetic long range order at sufficiently low temperature. For pressure below 60 GPa, both e_g and t_{2g} orbitals are insulating. In this case, the effective spin model describing the low energy physics will be the Heisenberg model with spin 3/2 on a fcc lattice, which leads to a ground state with antiferromagnetic (AFM) long-range order. However, after the OSMT at 60 GPa, the t_{2g} orbitals become metallic while the e_g orbitals remain insulating. In this particular case, the low energy effective model should be a double exchange model with itinerant t_{2g} orbitals and local moments sitting on e_g orbitals, which are coupled by Hund's rule coupling J. There is an interesting competition between the superexchange interactions among local moments on e_g orbitals which are antiferromagnetic, and the double exchange mechanism which obviously favors the ferromagnetic (FM) phase. Therefore, in low temperature there may be an AFM to FM transition accompanying the OSMT. The AFM long range order at CoO and its pressure dependence are a very interesting and important topic, so further calculations are essential and should be undertaken in the near future.

IV. CONCLUSION

In summary, we conclude that the two-step-like insulator-to-metal transition in CoO can be understood as a typical OSMT. At ambient pressure, CoO is a charge transfer insulator with an energy gap around 1.8 eV. At the first transition around 60 GPa, the t_{2g} bands become metallic while the e_g bands still remain insulating until the pressure reaches 170 GPa. Therefore, in CoO the intriguing OSMP with metallic t_{2g} and insulating e_g bands is stable in a quite large pressure window between 60 and 170 GPa. Our theoretical calculations also find that the Co^{2+} ions remain in HS states during the first transition and the crossover to the LS states starts only after the second transition. This is in good agreement with both the resistivity[16] and XES data[17,18] for CoO. Further analysis of the calculated results shows that the HS-LS transition is the main driving force of the Mott MIT in cubic CoO.

ACKNOWLEDGMENTS

We acknowledge financial support from the National Science Foundation of China and from the 973 program of China under Contracts No. 2007CB925000 and No. 2011CBA00108. All the LDA + DMFT calculations have been performed on the SHENTENG7000 at the Supercomputing Center of the Chinese Academy of Sciences (SCCAS).

[1]M. Imada, A. Fujimori, and Y. Tokura, Rev. Mod. Phys. **70**, 1039 (1998).
[2]V. I. Anisimov, I. A. Nekrasov, D. E. Kondakov, T. M. Rice, and M. Sigrist, Eur. Phys. J. B **25**, 191 (2002).
[3]A. Liebsch, Phys. Rev. Lett. **91**, 226401 (2003).
[4]A. Koga, N. Kawakami, T. M. Rice, and M. Sigrist, Phys. Rev. Lett. **92**, 216402 (2004).
[5]A. Koga, N. Kawakami, T. M. Rice, and M. Sigrist, Phys. Rev. B **72**, 045128 (2005).
[6]L. de'Medici, A. Georges, and S. Biermann, Phys. Rev. B **72**, 205124 (2005).
[7]L. de' Medici, S. R. Hassan, M. Capone, and X. Dai, Phys. Rev. Lett. **102**, 126401 (2009).
[8]P. Werner and A. J. Millis, Phys. Rev. Lett. **99**, 126405 (2007).
[9]J. Kuneš, A. V. Lukoyanov, V. I. Anisimov, R. T. Scalettar, and W. E. Pickett, Nat. Mater. **7**, 198 (2008).
[10]J. Kuneš, D. M. Korotin, M. A. Korotin, V. I. Anisimov, and P. Werner, Phys. Rev. Lett. **102**, 146402 (2009).
[11]A. O. Shorikov, Z. V. Pchelkina, V. I. Anisimov, S. L. Skornyakov, and M. A. Korotin, Phys. Rev. B **82**, 195101 (2010).
[12]I. S. Lyubutin, S. G. Ovchinnikov, A. G. Gavriliuk, and V. V. Struzhkin, Phys. Rev. B **79**, 085125 (2009).
[13]R. E. Cohen, I. I. Mazin, and D. G. Isaak, Science **275**, 654 (1997).
[14]A. G. Gavriliuk, V. V. Struzhkin, I. S. Lyubutin, S. G. Ovchinnikov, M. Y. Hu, and P. Chow, Phys. Rev. B **77**, 155112 (2008).
[15]A. Mattila, J.-P. Rueff, J. Badro, G. Vankó, and A. Shukla, Phys. Rev. Lett. **98**, 196404 (2007).
[16]T. Atou, M. Kawasaki, and S. Nakajima, Jpn. J. Appl. Phys. **43**, L1281 (2004).
[17]J.-P. Rueff, A. Mattila, J. Badro, G. Vank, and A. Shukla, J. Phys.: Condens. Matter **17**, S717 (2005).
[18]E. Z. Kurmaev, R. G. Wilks, A. Moewes, L. D. Finkelstein, S. N. Shamin, and J. Kuneš, Phys. Rev. B **77**, 165127 (2008).
[19]D. Kasinathan, J. Kuneš, K. Koepernik, C. V. Diaconu, R. L. Martin, I. D. Prodan, G. E. Scuseria, N. Spaldin, L. Petit, T. C. Schulthess, and W. E. Pickett, Phys. Rev. B **74**, 195110 (2006).
[20]U. Wdowik and D. Legut, J. Phys. Chem. Solids **69**, 1698 (2008).
[21]W. Zhang, K. Koepernik, M. Richter, and H. Eschrig, Phys. Rev. B **79**, 155123 (2009).
[22]A. Georges, G. Kotliar, W. Krauth, and M. J. Rozenberg, Rev. Mod. Phys. **68**, 13 (1996).
[23]G. Kotliar, S. Y. Savrasov, K. Haule, V. S. Oudovenko, O. Parcollet, and C. A. Marianetti, Rev. Mod. Phys. **78**, 865 (2006).
[24]D. Korotin, A. Kozhevnikov, S. Skornyakov, I. Leonov, N. Binggeli, V. Anisimov, and G. Trimarchi, Eur. Phys. J. B **65**, 91 (2008).
[25]G. Trimarchi, I. Leonov, N. Binggeli, D. Korotin, and V. I. Anisimov, J. Phys.: Condens. Matter **20**, 135227 (2008).
[26]B. Amadon, F. Lechermann, A. Georges, F. Jollet, T. O. Wehling, and A. I. Lichtenstein, Phys. Rev. B **77**, 205112 (2008).
[27]P. Giannozzi, S. Baroni, N. Bonini, M. Calandra, R. Car, C. Cavazzoni, D. Ceresoli, G. L. Chiarotti, M. Cococcioni, I. Dabo, A. Dal Corso, S. de Gironcoli, S. Fabris, G. Fratesi, R. Gebauer, U. Gerstmann, C. Gougoussis, A. Kokalj, M. Lazzeri, L. Martin-Samos, N. Marzari, F. Mauri, R. Mazzarello, S. Paolini, A. Pasquarello, L. Paulatto, C. Sbraccia, S. Scandolo, G. Sclauzero, A. P. Seitsonen, A. Smogunov, P. Umari, and R. M. Wentzcovitch, J. Phys.: Condens. Matter **21**, 395502 (2009).
[28]P. Werner, A. Comanac, L. de' Medici, M. Troyer, and A. J. Millis, Phys. Rev. Lett. **97**, 076405 (2006).
[29]E. Gull, A. J. Millis, A. I. Lichtenstein, A. N. Rubtsov, M. Troyer, and P. Werner, Rev. Mod. Phys. **83**, 349 (2011).
[30]V. I. Anisimov, J. Zaanen, and O. K. Andersen, Phys. Rev. B **44**, 943 (1991).
[31]L. Boehnke, H. Hafermann, M. Ferrero, F. Lechermann, and O. Parcollet, Phys. Rev. B **84**, 075145 (2011).
[32]M. Jarrell and J. Gubernatis, Phys. Rep. **269**, 133 (1996).
[33]M. D. Rechtin and B. L. Averbach, Phys. Rev. B **6**, 4294 (1972).
[34]K. S. D. Beach, arXiv:cond-mat/0403055.
[35]L. de' Medici, Phys. Rev. B **83**, 205112 (2011).